Particuology 10 (2012) 497–502

Contents lists available at SciVerse ScienceDirect

Particuology

journal homepage: www.elsevier.com/locate/partic

Size and shape effects on magnetic properties of Ni nanoparticles

Xuemin He, Huigang Shi*

Key Laboratory for Magnetism and Magnetic Materials of the Ministry of Education, Lanzhou University, Lanzhou 730000, China

A R T I C L E I N F O

Article history:
Received 1 July 2011
Received in revised form
14 November 2011
Accepted 21 November 2011

Keywords:
Precursor concentration
Size effect
Shape anisotropy
Curie temperature

A B S T R A C T

Pure Ni nanoparticles ranging in size from 24 to 200 nm are prepared via thermal decomposition of nickel acetylacetonate in oleylamine. The as-prepared Ni particles change from spherical to dendritic or starlike with increasing precursor concentration. The particles are stable because the organic coating occurs *in situ*. Magnetic measurement reveals that all the Ni nanoparticles are ferromagnetic and show ferromagnetic–paramagnetic transitions at their Curie points. The saturation magnetization M_s is size-dependent, with a maximum value of 52.01 and 82.31 emu/g at room temperature and 5 K, respectively. The coercivity decreases at first and then increases with increasing particle size, which is attributed to the competition between size effect and shape anisotropy. The Curie temperature T_c is 593, 612, 622, 626 and 627 K for the 24, 50, 96, 165 and 200 nm Ni nanoparticles, respectively. A theoretical model is proposed to explain the size-dependence of Ni nanoparticle Curie temperature.

1. Introduction

With the development of nanotechnology, more and more efforts have been directed toward the preparation of novel nanomaterials, with diverse applications. Among the transition metal magnetic particles, Ni nanoparticles have been extensively studied because of their multifarious uses including magnetic sensor (Wang et al., 2002), memory device (Zheng & Sun, 2006) and biomolecular separation (Lee, Park, & Mirkin, 2004). Purity, structure, size and shape of Ni nanoparticles greatly influence the ultimate performance of the materials and devices made of them. So it is significant to prepare high quality Ni nanoparticles by using a convenient and low-cost method. Recently, controlled synthesis of Ni nanoparticles has been achieved by various methods such as anodic arc plasma (Wei et al., 2006), chemical reduction (Bala et al., 2009; Margeat, Amiens, Chaudret, Lecante, & Benfield, 2005; Roy, Srinivas, Ram, & Chandrasekhar Rao, 2007; Tzitzios et al., 2006), pyrolysis (Che et al., 1999; Chen, Zhou, He, Chen, & Guo, 2010; Leng, Wang, Li, Liu, & Takahashhi, 2006), reversed micelle (Mandal, Kundu, Sau, Yusuf, & Pal, 2003) and polyol process (Chow et al., 1999).

However, pure Ni nanoparticles are difficult to prepare because they are easily oxidized. To obtain pure Ni nanoparticles, many methods are carried out in organic media to avoid the formation of oxide or hydroxide. For example, $Ni(COD)_2$ is used to synthesize Ni particles by spontaneous decomposition in CH_2Cl_2 in the presence of poly-vinylpyrrolidone (de Caro & Bradley, 1997; Ely et al., 1999). More interestingly, trigonal Ni nanoparticles were prepared by reacting $Ni(COD)_2$ in tetrahydrofuran with tetra-n-octylammonium carboxylates as a reductant and stabilizer (Bradley, Tesche, Busser, Maase, & Reetz, 2000). The above thermal decomposition method is convenient and easy to handle, and the use of organometallic precursors leads to particles with controlled size, shape, surface coordination and crystallinity.

This paper reports a facile and reproducible route to synthesize size- and shape-controlled Ni nanoparticles. The microstructure, chemical stability and magnetic properties of the as-synthesized Ni particles are studied in detail. We focus on the influence of particle size and shape on saturation magnetization, coercivity and Curie temperature. Especially, the size dependence of Curie temperature can be explained via a theoretical model.

2. Experimental

2.1. Sample preparation

Ni nanoparticles were prepared by the pyrolysis method. In a typical synthesis process, nickel(II) acetylacetonate $[Ni(acac)_2]$ (0.39 g, 1.50 mmol) and oleylamine (98.70 mL, 300.00 mmol) were mixed and stirred in a three-necked flask. The mixture was heated at 135 °C in an oil bath for 15 min under an argon atmosphere, resulting in an emerald solution. Following this dissolution, the solution was heated up to 245 °C at a rate of 8 °C/min, and was kept at this temperature for 1 h. Then, the reaction mixture was

---

* Corresponding author. Tel.: +86 931 8912688; fax: +86 931 8914160.
E-mail addresses: shihuig@lzu.edu.cn, zspohexuemin@163.com (H. Shi).

1674-2001/$ – see front matter © 2012 Chinese Society of Particuology and Institute of Process Engineering, Chinese Academy of Sciences. Published by Elsevier B.V. All rights reserved.
doi:10.1016/j.partic.2011.11.011

Table 1
Particle size (D), Curie temperature (T_c), saturation magnetization (M_s) and coercivity (H_c) for the Ni samples synthesized at different precursor concentrations (C).

Sample	C	D (nm)	T_c (K)	M_s (emu/g)		H_c (Oe)	
				300 K	5 K	300 K	5 K
M1	1/200	24	593	25.25	50.19	120	287
M2	1/100	50	612	32.30	53.49	79	250
M3	1/50	96	622	40.59	57.03	18	230
M4	1/20	165	626	46.66	64.77	146	379
M5	1/10	200	627	52.01	82.31	158	403

cooled down to room temperature and a black colloidal solution was obtained. The black precipitate was separated upon the addition of ethanol and hexane, centrifuged, and then washed using a mixture of ethanol and toluene. At the end, the black Ni particles (sample M1) were dried in an oven at room temperature overnight. Under similar reaction conditions, other four Ni samples (M2–M5) with various particle sizes were produced by simply changing the precursor concentration (the molar ratio of Ni(acac)$_2$ and oleylamine), as shown in Table 1.

2.2. Characterization

Powder X-ray diffraction (XRD) patterns were obtained with a Rigaku D/Max-2400 diffractometer equipped with a rotating anode and Cu Kα radiation ($\lambda = 0.15418$ nm). Particle size and morphology were examined by a Hitachi S-4800 scanning electron microscope (SEM) with an accelerating voltage of 5 kV. Absorption spectra were recorded from 400 to 4000 cm^{-1} on a Nexus 670 Fourier transform infrared (FTIR) spectrometer. Room temperature hysteresis loops and magnetization versus temperature curves were measured with a Lake Shore 7304 vibrating sample magnetometer (VSM), and 5 K hysteresis loops were obtained with a MPMS-XL superconducting quantum interference device (SQUID) magnetometer.

3. Results and discussion

Fig. 1 shows typical XRD patterns of the solid samples obtained under different precursor concentrations, showing that the five samples are all Ni particles. All the peaks of the five patterns are well indexed as cubic Ni phase with face-centered cubic (fcc) structure. Three obvious Bragg peaks ($2\theta = 44.54^\circ, 51.86^\circ, 76.51^\circ$) can be assigned to scattering from the (1 1 1), (2 0 0) and (2 2 2) planes of the Ni crystal lattice, respectively. The peaks are observably broadened with decreasing precursor concentration. By making use of the line width, the particle size D can be estimated using Scherrer formula. As shown in Table 1, the particle sizes of the five samples were found to be 24, 50, 96, 165 and 200 nm, respectively.

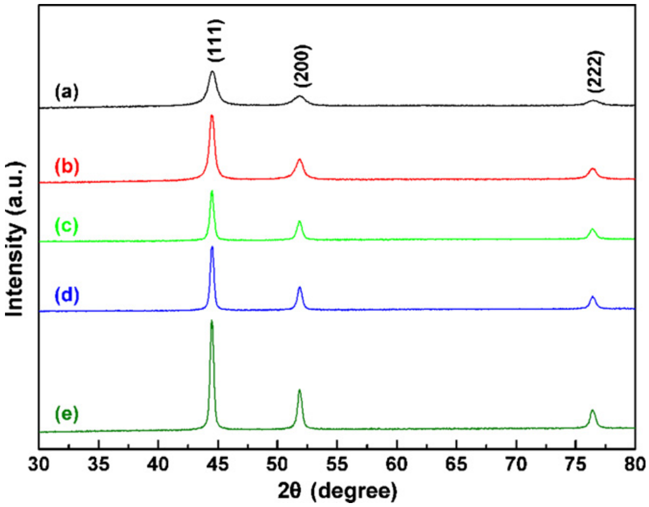

Fig. 1. XRD patterns of Ni nanoparticles formed in different precursor concentrations: (a) 1/200, (b) 1/100, (c) 1/50, (d) 1/20 and (e) 1/10.

Fig. 2 shows the representative SEM images of the as-synthesized Ni nanoparticles obtained under different precursor concentrations. Obviously, the average size of Ni particles increases with increasing precursor concentration, and the particle shape also changes from spherical (Fig. 2(a)–(c)) to dendritic (Fig. 2(d)) or starlike (Fig. 2(e)). The size distributions of the spherical samples M1–M3 are also shown respectively in Fig. 2(a1)–(c1). Their average particle size was observed to be 24.6, 48.9 and 94.8 nm, respectively, in excellent agreement with the results of XRD analyses. It can be seen that the standard deviations of particle size are less than 10% for the three samples. Further, increase of particle size deteriorates the uniformity of the size distribution, implying that the different concentration of oleylamine will cause different density of organic functional groups on the particle surface, which may be the direct reason for easy control over the particle size and size distribution during the growth process. Therefore, the size and shape of Ni nanoparticles are well controlled by changing the precursor concentration.

Fig. 3 shows a typical FTIR spectrum of Ni nanoparticles with an average diameter of 96 nm. The peaks at 2853.8 and 2923.1 cm^{-1} are due to the symmetric and asymmetric CH$_2$ stretching modes, the peak at 3005.9 cm^{-1} is due to the n(C–H) mode of the C–H bond adjacent to the C=C bond, and the peak at 1626.2 cm^{-1} is due to the n(C=C) stretching mode. In addition, the small peak at 1593.0 cm^{-1} is due to the NH$_2$ scissoring mode (Shukla, Liu, Jones, & Weller, 2003). The results clearly reveal that the nanoparticles are coated with the oleylamine, which prevents them from being oxidized by oxygen.

Fig. 4(a) and (c) depict the hysteresis loops of the as-synthesized Ni nanoparticles with different particle sizes at room temperature and 5 K, respectively. All the samples show ferromagnetic behavior with coercivity H_c and magnetic remanence M_r. With increasing particle sizes, the magnetization of the samples increases quickly with applied field. As shown in Table 1, the saturation magnetization M_s increases monotonously with the increase of particle size. At 300 and 5 K, the maximum value of M_s is 52.01 and 82.31 emu/g, respectively. In order to explain the phenomenon that the saturation magnetization decreases with decreasing particle size in proportion to their specific surface area, a magnetically dead layer theory was developed (Kodama, 1999). As the surface-to-volume ratio increases with decreasing particle size, the magnetically inactive layer fraction increases, too. Therefore, the saturation magnetization M_s of Ni nanoparticles decreases with the decrease of particle size.

Fig. 4(b) and (d) also shows the size dependence of the coercivity H_c at 300 and 5 K, respectively. Obviously, H_c decreases at first and then increases with the increase of particle size D. In our opinion, two main factors relate to coercivity: particle size and shape anisotropy. It is well known that H_c of ferromagnetic nanoparticles with regular shape conforms to the rule of $H_c \propto 1/D$. Therefore, for the spherical samples M1–M3, the larger the particle size, the lower the coercivity. While for the dendritic sample M4 with a particle size of 165 nm and the starlike sample M5 with a particle size of 200 nm, their coercivities become larger rather than smaller, indicating that the influence of shape anisotropy is dominant at this time. The relationship of $H_c \propto \Delta N M_s$ (where ΔN is the diversity of demagnetization factor in different directions) explains why samples M4 and M5 have large coercivities. In a word, the change of H_c is largely attributed to the size and shape effects. Based on the